JACS
JOURNAL OF THE AMERICAN CHEMICAL SOCIETY
Article
pubs.acs.org/JACS

The Hexachlorocerate(III) Anion: A Potent, Benchtop Stable, and Readily Available Ultraviolet A Photosensitizer for Aryl Chlorides

Haolin Yin,[†] Yi Jin,[†] Jerald E. Hertzog,[†,§] Kimberly C. Mullane,[†] Patrick J. Carroll,[†] Brian C. Manor,[†] Jessica M. Anna,*[,†] and Eric J. Schelter*[,†]

[†]P. Roy and Diana T. Vagelos Laboratories, Department of Chemistry, University of Pennsylvania, 231 South 34 Street, Philadelphia, Pennsylvania 19104, United States

[§]Department of Chemistry, Washington & Jefferson College, 60 S Lincoln Street, Washington, Pennsylvania 15301, United States

Supporting Information

ABSTRACT: The hexachlorocerate(III) anion, $[Ce^{III}Cl_6]^{3-}$, was found to be a potent photoreductant in acetonitrile solution with an estimated excited-state reduction potential of −3.45 V versus $Cp_2Fe^{0/+}$. Despite a short lifetime of 22.1(1) ns, the anion exhibited a photoluminescence quantum yield of 0.61(4) and fast quenching kinetics toward organohalogens allowing for its application in the photocatalytic reduction of aryl chloride substrates.

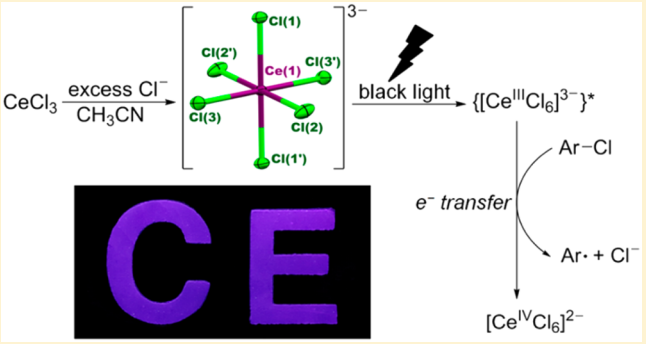

1. INTRODUCTION

The direction of light energy for organic transformations relies on the ability to photochemically generate important radical intermediates[1−7] such as aryl radicals.[8,9] The scission of C−X bonds (X = Cl, Br, I) in aryl halide substrates can be directly achieved under photolysis conditions to afford the corresponding aryl radicals.[10] However, the direct $\pi-\pi^*$ excitation of aryl halides requires high energy and carcinogenic ultraviolet C (UVC) light (100−280 nm),[11,12] which is only a small portion of solar spectrum.[13,14] Alternatively, lower energy ultraviolet A (UVA light or black light, 315−400 nm) and visible light can be converted into chemical reduction potential using molecular photosensitizers to mediate single electron reduction reactions of aryl iodides and bromides.[15−23] For example, photoexcited *fac*-$Ir(ppy)_3$ (ppy = 2,2′-phenylpyridine) is capable of reducing unactivated aryl iodides,[15,16] and luminescent dinuclear gold(I) and copper(I) complexes were applied as triplet photoreductants for aryl bromides under UVA light.[17−19] In contrast, aryl chloride substrates are not accessible substrates in such transformations due to their large negative reduction potentials.

The $PhCl^{\bullet-}$/PhCl redox couple was reported at −3.28 V versus $Cp_2Fe^{0/+}$ in dimethylformamide (DMF),[24] exceeding the excited-state reduction potentials of the most potent molecular photoreductants reported to date.[25−27] A double excitation process of pyrene bisimide (PDI) derivatives with visible light[28] or excitation of 10-phenylphenothiazine with UVA light (380 nm)[29] was necessary to accumulate sufficient chemical potential for the reduction of aryl chlorides bearing electron withdrawing substituents. Compared to aryl bromides and iodides, aryl chlorides are more attractive substrates in terms of their cost and availability. Therefore, the development of more potent photoreductants is at the crux of engaging unactivated aryl chlorides in photochemical reactions. Following from the requisite reduction potential of aryl chlorides, the maximum wavelength of light required for aryl chloride activation would be 375 nm (assuming ground-state reduction potential of the photosensitizer at 0 V versus $Cp_2Fe^{0/+}$), meaning a thermodynamic requirement for UVA light.

Our group has been developing molecular photosensitizers[27,30] with the earth abundant element cerium.[31] The cost of cerium salts is favorable compared to ruthenium, iridium, and gold photosensitizers. Upon excitation to their long-lived ^2D excited states, the redox active Ce^{3+} cations[32] behave as d-block-type metalloradicals and readily engage in single electron transfer (SET) reactions. A further advantage of cerium photosensitizers is the conservation of spin state in their excited states,[33] which avoids energy losses through intersystem crossing (ISC) processes. This is in sharp contrast to transition metal photosensitizers, including Cr^{III}, W^0, Ru^{II}, Ir^{III}, Au^{I}, and Cu^{I} complexes.[16−18,20,26,34−38] In previous studies, we demonstrated brightly luminescent Ce^{III} complexes with amide and guanidinate ligands as molecular photoreductants to effect organic transformations using visible light irradiation.[27,30] In particular, $Ce^{III}[N(SiMe_3)_2]_3$, a common Ce^{III} protonolysis reagent, was shown to mediate single electron transfer toward $PhCH_2Cl$, aryl bromide, and aryl iodide substrates.[30] However, these Ce^{III} photosensitizers were not capable of reducing aryl chloride

Received: June 3, 2016
Published: November 22, 2016

DOI: 10.1021/jacs.6b05712
J. Am. Chem. Soc. 2016, 138, 16266−16273

substrates. The air and moisture sensitivity of the organocerium(III) photosensitizers also poses difficulty in their storage and convenient application.

In the current work, we report studies of a UVA photoreductant, the hexachlorocerate(III), $[Ce^{III}Cl_6]^{3-}$, anion. The $[Ce^{III}Cl_6]^{3-}$ anion is stable to oxygen and moisture either in the solid state or in acetonitrile solution and thus can be stored on the benchtop. This trianionic species can be readily generated *in situ* from $CeCl_3$ and NEt_4Cl in acetonitrile solutions. We demonstrate that the low photoreduction potential and fast quenching kinetics of $[Ce^{III}Cl_6]^{3-}$ enable facile dehalogenation reactions of aryl chloride substrates.

2. RESULTS AND DISCUSSION

2.1. Synthesis and Characterization. Costanzo and coworkers previously noted the photoreduction of cerium(IV) hexachloride ($[Ce^{IV}Cl_6]^{2-}$) species in acetonitrile, leading to the formation of cerium(III) species.[39] Following their report, we developed a new procedure for the preparation of $[NEt_4]_3[Ce^{III}Cl_6]$ in 81% isolated yield in a mixture of toluene and acetonitrile from $[NEt_4]_2[Ce^{IV}Cl_6]$ using visible light irradiation (Scheme 1). The organic byproduct was determined

Scheme 1. Synthesis of $[NEt_4]_3[Ce^{III}Cl_6]$ through a Photochemical Method

$$[NEt_4]_2[Ce^{IV}Cl_6] \xrightarrow[\text{visible light CFLs}\ N_2,\ \text{r.t.}]{\text{1 eq } NEt_4Cl,\ \text{toluene/}CH_3CN\ (1:4)} [NEt_4]_3[Ce^{III}Cl_6]$$

by gas chromatography (GC) to be primarily $PhCH_2Cl$ (~0.5 equiv) with trace amounts of $PhCH_2CH_2Ph$. An X-ray crystallography study on the crystals of $[NEt_4]_3[Ce^{III}Cl_6]$ obtained from CH_3CN/Et_2O vapor diffusion revealed the expected octahedral $[Ce^{III}Cl_6]^{3-}$ structure with an average Ce−Cl bond length of 2.7797(7) Å. The ~0.15 Å increase in the average Ce−Cl bond length compared to $[Ce^{IV}Cl_6]^{2-}$ (2.6084(7) Å) was consistent with the difference in the ionic radius between six-coordinate Ce^{3+} and Ce^{4+} cations.[40] The data for $[NEt_4]_3[Ce^{III}Cl_6]$ was also consistent with previous structural determinations.[41,42]

The emission spectrum of $[NEt_4]_3[Ce^{III}Cl_6]$ recorded in CH_3CN featured three maxima at 356, 395, and 442 nm, indicative of multiple Ce^{III} containing species in solution (Figure 1, green dashed trace). Upon addition of excess (≥10 equiv) NEt_4Cl to $[NEt_4]_3[Ce^{III}Cl_6]$ in CH_3CN, a single emissive cerium(III) species was observed (Figure 1, blue dashed trace); the resulting emission spectrum could be deconvoluted into two Gaussian bands separated by 2243 cm^{-1} (Figure S11). The two bands were consistent with emissive transitions from a single long-lived excited state to the $^2F_{5/2}$ and $^2F_{7/2}$ states of a Ce^{3+} cation.[43−47] Both emission bands in the blue trace were confirmed to originate from the $[Ce^{III}Cl_6]^{3-}$ anion through comparison of the solution emission spectra with solid-state photoluminescence spectrum of $[NEt_4]_3[Ce^{III}Cl_6]$ (Figure S12) and the reported $[BMIM]_3[Ce^{III}Cl_6]$ ($[BMIM]^+$ = 1-butyl-3-methylimidazolium).[42] More conveniently, the $[Ce^{III}Cl_6]^{3-}$ species could also be accessed by dissolving $CeCl_3$ in CH_3CN in the presence of 15 equiv of NEt_4Cl, as monitored in the emission spectrum (Figure S15). The other major Ce^{3+} containing species in the absence of additional NEt_4Cl was identified as the $[Ce_2Cl_9]^{3-}$ anion: crystalline $[NEt_4]_3[Ce_2Cl_9]$ could be prepared from $CeCl_3$ and $[NEt_4]_3[CeCl_6]$ (see Supporting Information) and demonstrated a simple emission spectrum (Figure 1, yellow dashed trace). However, the possibility of forming oligomeric Ce^{3+} containing species in addition to $[Ce_2Cl_9]^{3-}$ in the absence of excess Cl^- anion was not excluded.

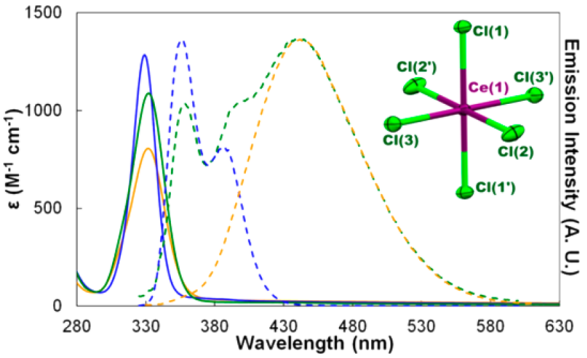

Figure 1. Absorption (solid lines) and emission (dashed lines) spectra for an acetonitrile solution of $[NEt_4]_3[Ce^{III}Cl_6]$ (green traces), $[NEt_4]_3[Ce^{III}Cl_6]$ in the presence of excess NEt_4Cl (blue traces, 2 mM $[NEt_4]_3[Ce^{III}Cl_6]$ and 0.1 M NEt_4Cl), and $[NEt_4]_3[Ce_2Cl_9]$ (yellow traces). X-ray molecular structure of the $[Ce^{III}Cl_6]^{3-}$ anion is shown in the inset. Cations are omitted for clarity.

The electronic absorption spectrum of $[Ce^{III}Cl_6]^{3-}$ (Figure 1, blue solid trace) demonstrated one transition at 329 nm with $\varepsilon \approx 1.3 \times 10^3$ M^{-1} cm^{-1} and a full width at half maxima (fwhm) of 1762 cm^{-1}. This absorptive band was assigned using time-dependent density functional theory (TD-DFT) to be an interconfigurational transition from a state corresponding to the Ce^{III} 4f orbitals to a state corresponding to Ce−Cl π-antibonding orbitals with predominant Ce^{III} $5d_{xy}$, $5d_{yz}$, and $5d_{xz}$ character ($^2T_{2g}$* in idealized O_h symmetry, Figure S23), consistent with the previous assignment by Ryan and Jørgensen.[48] The excitation spectrum of the $[Ce^{III}Cl_6]^{3-}$ anion demonstrated an intense band, overlapping with the lowest energy absorption band at 329 nm. This result allowed us to conclude that the $^2T_{2g}$* excited state of the octahedral $[Ce^{III}Cl_6]^{3-}$ species corresponded to the long-lived excited state. The photoluminescence quantum yield and lifetime (τ_0) were determined for the $[Ce^{III}Cl_6]^{3-}$ anion to be 0.61(4) and 22.1(1) ns (Figure S25) in 0.1 M NEt_4Cl acetonitrile solution, respectively. The observed lifetime for $[Ce^{III}Cl_6]^{3-}$ was consistent with that reported for Ce^{3+} cations doped in chloroelapsolite, Cs_2NaYCl_6 (30 ns at 77 K).[49,50]

2.2. Estimated Excited-State Reduction Potential and Quenching Kinetics. The small Stokes shift of 27 nm (0.30 eV) observed for $[Ce^{III}Cl_6]^{3-}$ implied that most energy of the UVA light absorbed by the photosensitizer was conserved in its $^2T_{2g}$* excited state. A cyclic voltammetry experiment on $[NEt_4]_3[Ce^{III}Cl_6]$ in CH_3CN using 0.1 M NEt_4Cl as supporting electrolyte revealed a simple $[Ce^{III}Cl_6]^{3-}/[Ce^{IV}Cl_6]^{2-}$ redox couple with $E_{1/2}$ = +0.03 V versus $Cp_2Fe^{0/+}$ (Figure S6). In contrast, when $[N^nBu_4][PF_6]$ was used as supporting electrolyte, multiple cathodic waves were observed (Figure S8). This result is consistent with the solution speciation for $[NEt_4]_3[Ce^{III}Cl_6]$ in acetonitrile solution in the absence of excess Cl^-.

Combining the ground-state electrochemical data and spectroscopic data, we estimated the excited-state reduction potential ($E_{1/2}$*) of $[Ce^{III}Cl_6]^{3-}$ species to be −3.45 V versus $Cp^2Fe^{0/+}$ following the Rehm−Weller formalism:[51,52]

$$E_{1/2}^* = E_{1/2} - E_{0,0} + \omega$$

DOI: 10.1021/jacs.6b05712
J. Am. Chem. Soc. 2016, 138, 16266−16273

Table 1. Comparison of Substrate Quenching Rates (k_q) and Decay Rates (k_d) of Photosensitizers toward $PhCH_2Cl$ and Aryl Halide Substrates

photosensitizer	substrate	solvent	k_q, M^{-1} s^{-1}	k_d, s^{-1}	K_{SV}, M^{-1}
$[Ce^{III}Cl_6]^{3-}$	$PhCH_2Cl$	CH_3CN	3.2×10^9	4.5×10^7	71
$[Au_2(\mu\text{-dppm})_3]^{2+}$	$PhCH_2Cl$	CH_3CN	1.9×10^6	4.8×10^4	39
$Cu(dap)_2^+$	$PhCH_2Br$	CH_2Cl_2	5.0×10^6	3.7×10^6	1.4
$[Ce^{III}Cl_6]^{3-}$	4−F-C_6H_4I	CH_3CN	1.1×10^{10}	4.5×10^7	244
$Ce[N(SiMe_3)_2]_3$	4−F-C_6H_4I	toluene	2.1×10^9	4.2×10^7	50
$[(Me_3Si)_2NC(N^iPr)_2]Ce[N(SiMe_3)_2]_2$	4−F-C_6H_4I	toluene	2.2×10^8	1.5×10^7	15
$[(Me_3Si)_2NC(N^iPr)_2]_2Ce[N(SiMe_3)_2]$	4−F-C_6H_4I	toluene	1.9×10^7	8.5×10^6	2.2
$[(Me_3Si)_2NC(N^iPr)_2]_3Ce$	4−F-C_6H_4I	toluene	3.5×10^7	1.2×10^7	2.9
$[Ce^{III}Cl_6]^{3-}$	4−F-C_6H_4Br	CH_3CN	3.0×10^9	4.5×10^7	67
$[Ce^{III}Cl_6]^{3-}$	4−F-C_6H_4Cl	CH_3CN	2.7×10^9	4.5×10^7	60
$[Ce^{III}Cl_6]^{3-}$	4−F-C_6H_4F	CH_3CN	9.3×10^8	4.5×10^7	21

where $E_{1/2}$ is the ground-state reduction potential; $E_{0,0}$ is the energy difference between zeroth vibrational states of the ground and electronic excited states and can be approximated by the emission energy (3.48 eV). The work function ω is usually a small contribution and was omitted here (see Supporting Information for details). On the other hand, the reduction of CH_3CN does not occur until −3.5 V versus $Cp_2Fe^{0/+}$,[53] allowing for the use of $[Ce^{III}Cl_6]^{3-}$ anions as photoreductants in acetonitrile solution.

Solid $[NEt_4]_3[Ce^{III}Cl_6]$ and acetonitrile solution containing $[Ce^{III}Cl_6]^{3-}$ anions can be stored in air indefinitely in the absence of UVA light (Figure S47, S59). The $[Ce^{III}Cl_6]^{3-}$ species is also unreactive toward other weak oxidants, including Ph_3CCl, C_2Cl_6, and $PhCH_2Cl$. However, irradiation of an acetonitrile solution containing $[Ce^{III}Cl_6]^{3-}$ species and an excess of $PhCH_2Cl$ (E_{pc} = −2.66 V versus $Cp_2Fe^{0/+}$ in DMF)[54] under an N_2 atmosphere in a photoreactor equipped with 352 nm narrow band fluorescent tubes led to a color change to yellow. An electronic absorption spectrum of the reaction mixture confirmed the formation of $[Ce^{IV}Cl_6]^{2-}$ with a broad (fwhm = 5516 cm^{-1}) absorption feature centered at 378 nm (Figure S34). This band for $[Ce^{IV}Cl_6]^{2-}$ species was assigned as ligand-to-metal charge transfer (LMCT) transition. The orbital contributions to this LMCT transition were revealed by TD-DFT calculation to be from linear combinations of Cl 2p orbitals (t_{1g} in idealized O_h symmetry) to Ce^{IV} 4f orbitals (Figure S22), consistent with a recent report of the electronic structure of $[Ce^{IV}Cl_6]^{2-}$.[41] The organic product of the UVA irradiation of $[Ce^{III}Cl_6]^{3-}$ and $PhCH_2Cl$ was determined to be $PhCH_2CH_2Ph$ using ^1H NMR spectroscopy and gas chromatography mass spectrometry (GC-MS, Figure S33, S35). In contrast, no reaction was observed in the absence of $[Ce^{III}Cl_6]^{3-}$ or in the dark (Figure S36, S38). The above results were consistent with the formation of a benzyl radical intermediate through the photoreduction of $PhCH_2Cl$ by $[Ce^{III}Cl_6]^{3-}$.

The capability of photoexcited $[Ce^{III}Cl_6]^{3-}$ to reduce $PhCH_2Cl$ was also enhanced by its fast quenching kinetics. Upon addition of $PhCH_2Cl$, the photoluminescence intensity from $[Ce^{III}Cl_6]^{3-}$ species decreased. A rate constant of 3.2×10^9 M^{-1} s^{-1} was measured for the quenching process through Stern−Volmer experiments (Table 1). Importantly, the observed quenching rate (k_q) was faster than $k_q = 1.9 \times 10^6$ M^{-1} s^{-1} reported for the quenching process for $[Au_2(dppm)_3]^{2+}$ [dppm = bis(diphenylphosphino)methane][17,18] by $PhCH_2Cl$ in acetonitrile and $k_q = 5.0 \times 10^6$ M^{-1} s^{-1} reported for $Cu(dap)_2^+$ (dap = 2,9-bis(*p*-anisyl)-1,10-phenanthroline) by $PhCH_2Br$ in CH_2Cl_2.[37] Such high quenching rates observed for $[Ce^{III}Cl_6]^{3-}$ suggested effective, diffusion controlled, intermolecular deactivation of the metal centered excited state, likely enabled by its strong thermodynamic driving force for electron transfer to quencher molecules (see Supporting Information for details). Direct comparison of substrate quenching rates (k_q) with regard to decay rates ($k_d = \tau_0^{-1}$) of different photosensitizers was enabled by comparison of the Stern−Volmer constants (K_{SV}):

$$K_{SV} = k_q\tau_0 = k_q/k_d$$

A larger k_q/k_d ratio implied that the photosensitizer interacted more readily with the quenchers within the lifetime of their excited states (see Supporting Information). The K_{SV} value was calculated to be 71 M^{-1} for quenching of the $[Ce^{III}Cl_6]^{3-}$ $^2T_{2g}$* excited state with $PhCH_2Cl$, larger than that found for $[Au_2(\mu\text{-dppm})_3]^{2+}$ with $PhCH_2Cl$ (K_{SV} = 39 M^{-1}) and $Cu(dap)_2^+$ with $PhCH_2Br$ (K_{SV} = 1.4 M^{-1}). Importantly, fast quenching kinetics was also found for aryl halide substrates with $[Ce^{III}Cl_6]^{3-}$ (Table 1). The calculated K_{SV} for the quenching processes with 4-fluoroiodobenzene of $[Ce^{III}Cl_6]^{3-}$ was 244 M^{-1}, much faster than that observed previously with $Ce[N(SiMe_3)_2]_3$ (K_{SV} = 50 M^{-1}) and $[(Me_3Si)_2NC(N^iPr)_2]_3Ce$ (K_{SV} = 2.9 M^{-1}).[27] Similarly, a large k_q/k_d ratio (K_{SV} = 60 M^{-1}) was also found for $[Ce^{III}Cl_6]^{3-}$ and 4-chlorofluorobenzene substrates. This result, together with its $E_{1/2}$* = −3.45 V, prompted us to investigate the photochemical reaction between $[Ce^{III}Cl_6]^{3-}$ and aryl chloride substrates.

2.3. Photoinduced Dehalogenation Reactions of Ar−X (X = Cl, Br, I). In addition to dissolving premade $[NEt_4]_3[Ce^{III}Cl_6]$ in acetonitrile solution in the presence of excess NEt_4Cl, the $[Ce^{III}Cl_6]^{3-}$ anion could be readily generated *in situ* from a mixture of $CeCl_3$ and NEt_4Cl (Figure S15).[48] Therefore, we sought to apply $CeCl_3$ as a commercially available and low cost precursor in developing a simple protocol for the photochemical dehalogenation reactions of aryl halides.

Irradiation of a dilute acetonitrile solution containing $CeCl_3$ and 1 equiv of 4-chlorofluorobenzene in the presence of excess NEt_4Cl using commercial "black light" compact fluorescent lamps for 40 h resulted in the gradual formation of yellow $[Ce^{IV}Cl_6]^{2-}$ species. Analysis of the organic products by ^{19}F NMR spectroscopy revealed the production of fluorobenzene as the single product in 67% yield (Table 2, entry 1, Figure S49). The hydrogen atom in the dehalogenation product was determined to originate from the solvent: the mass of 4-deuterofluorobenzene and 4-fluorobenzene were identified by GC-MS for the reactions carried out in CD_3CN and in CH_3CN, respectively (Figure S41, S42). The yield of fluorobenzene increased with prolonged irradiation time (entries 2 and 3). Such

DOI: 10.1021/jacs.6b05712
J. Am. Chem. Soc. 2016, 138, 16266−16273

Table 2. Reductive Dehalogenation of Aryl Halide Substrates by $[Ce^{III}Cl_6]^{3-}$ Promoted by UVA Light

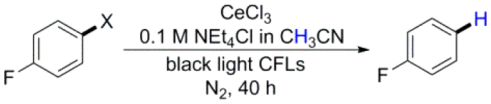

entry	X	variations from standard conditions[a]	yield[b] (%)
1	Cl	none	67(69[c])
2	Cl	72 h instead of 40 h	77(81[c])
3	Cl	104 h instead of 40 h	84
4	Cl	no $CeCl_3$	*d*
5	Cl	$LaCl_3$ instead of $CeCl_3$	*d*
6	Cl	$[NEt_4]_3[CeCl_6]$	65
7	Cl	$Ce(OTf)_3$ instead of $CeCl_3$	70
8	Cl	no NEt_4Cl	*d*
9	Cl	$CeCl_3{\cdot}7H_2O$ instead of $CeCl_3$	52
10	Cl	$NEt_4Cl{\cdot}H_2O$ instead of NEt_4Cl	45
11	Cl	$CeCl_3{\cdot}7H_2O$ instead of $CeCl_3$, $NEt_4Cl{\cdot}H_2O$ instead of NEt_4Cl	36
12	Cl	in the dark instead of UVA light	*d*
13	Cl	visible light CFL instead of black light	10
14	F	none	*d*
15	Br	none	87[c]
16	I	none	>95[c]
17	Br	$CeBr_3$ and NEt_4Br	12

[a]Standard conditions: 0.2 mmol of substrate, 0.2 mmol of $CeCl_3$, 30 mL CH_3CN solution of 0.1 M NEt_4Cl irradiated by two 23 W black light compact fluorescent lamps, 40 h. [b]Yield determined by ^{19}F NMR integrated using *p*-fluorotoluene as internal standard. [c]Reaction conducted in quartz glass bombs. [d]No reaction.

slow overall reactions were attributed to the absorptivity intrinsic to the Ce^{3+} cations. The extinction coefficient for the interconfigurational 4f → 5d absorptive transition is 10^2–10^3 M^{-1} cm^{-1}, orders of magnitude smaller than a typical LMCT transition (10^4–10^5 M^{-1} cm^{-1}). The dehalogenation reactions were found to proceed through aryl radical intermediates: the same reaction carried out in the presence of 200 equiv of benzene for 72 h resulted in the formation of 4-fluorobiphenyl in 28% yield, likely through the addition of aryl radical to benzene (Table S8).

A variety of control experiments suggested that $[Ce^{III}Cl_6]^{3-}$ was essential and UVA light was important for the dehalogenation reaction. No reaction occurred in the absence of either $CeCl_3$ (entry 4) or Cl^- anions (entry 8). The dehalogenation reaction did not occur with $LaCl_3$ (entry 5) despite the similar ionic radius between La^{3+} and Ce^{3+} cations. This result is consistent with our assignment that photochemical reaction of the $[Ce^{III}Cl_6]^{3-}$ anion occurred through metal centered 4f → 5d transitions instead of LMCT transitions. The use of other Ce^{3+} sources, such as $Ce(OTf)_3$ and $[NEt_4]_3[Ce^{III}Cl_6]$ also afforded the dehalogenation products in comparable yields to $CeCl_3$ (entries 6 and 7). The dehalogenation reaction did not proceed in the absence of UVA light (entries 12 and 13). The yields of dehalogenation products were also found to increase with the use of quartz reaction vessels instead of Pyrex glass bombs (entries 1 and 2). When the reaction was carried out with intermittent UVA light, no product formation was observed during the dark periods (Figure S50). This result indicated that the formation of the dehalogenation product was subject to temporal control, though a radical propagation process was not precluded.[55] Importantly, we found that the dehalogenation reactions proceeded even in the presence of a large amount of H_2O (7, 15, and 22 equiv in entries 9, 10, and 11, respectively) despite relatively lower yields compared to those under anhydrous conditions. The $[Ce^{III}Cl_6]^{3-}$ species in its $^2T_{2g}$* excite state was incapable of reducing aryl fluoride substrates (entry 14). For aryl bromide and aryl iodide substrates, the same reaction conditions could be directly employed to afford dehalogenation products in high yields (entries 15 and 16).

We attempted to extend the photochemical reactivity of $[Ce^{III}Cl_6]^{3-}$ to $[Ce^{III}Br_6]^{3-}$ species. Crystals of $[NEt_4]_3[Ce^{III}Br_6]$ could be afforded in 75% yield from $CeBr_3$ and 3 equiv of NEt_4Br (Figure 2, inset). And the corresponding $[Ce^{III}Br_6]^{3-}$ species

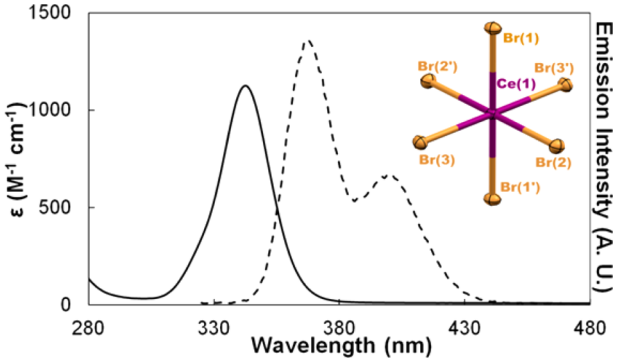

Figure 2. Absorption (black solid lines) and emission (black dashed lines) spectra for an acetonitrile solution of $[Ce^{III}Br_6]^{3-}$ (2 mM $[NEt_4]_3[Ce^{III}Br_6]$ and 0.1 M NEt_4Br). X-ray molecular structure of the $[Ce^{III}Br_6]^{3-}$ anion is shown in the inset. Cations are omitted for clarity.

demonstrated absorption and emission features similar to $[Ce^{III}Cl_6]^{3-}$ (Figure 2) with absorption and emission maxima at 343 and 367 nm, respectively. The lifetime for $[Ce^{III}Br_6]^{3-}$ was determined to be 35.5(1) ns in 0.1 M NEt_4Br acetonitrile solution (Figure S26). When the debromination reaction was conducted with $[Ce^{III}Br_6]^{3-}$, only a low yield of fluorobenzene was observed (entry 17), likely due to the instability of the corresponding $[Ce^{IV}Br_6]^{2-}$ species. Cyclic voltammetry experiments revealed that the Br^- oxidation[56] occurred prior to the $[Ce^{III}Br_6]^{3-}/[Ce^{IV}Br_6]^{2-}$ couple in CH_3CN, consistent with the reports of $[Ce^{IV}Br_6]^{2-}$ being a transient species in the presence of excess Br^- at room temperature.[48]

The photochemical dechlorination reaction with $CeCl_3$ was applicable toward a variety of aryl chloride and bromide substrates and functional groups, including methoxy, silyloxy, trifluoromethyl, and cyano groups (Table 3). Moderate yields of dehalogenation products could be obtained after 3 days even for aryl chloride substrates with electron donating groups, indicating the low reduction potential of $[Ce^{III}Cl_6]^{3-}$ in its $^2T_{2g}$* excited state. The relatively low yields observed for aryl chlorides with electron donating substituents were attributed to the associated slow electron transfer processes. In particular, the reaction with 1-*tert*-butyl-4-chlorobenzene substrate only resulted in a low yield of 34% without noticeable byproduct formation. This result is consistent with the expectation that electron rich aryl rings are less efficient electron acceptors. In comparison, higher yields of dehalogenation products were achieved with corresponding aryl bromide substrates under the same condition. This result is consistent with aryl bromides being more susceptible to reduction than aryl chlorides.[24] Moreover, aryl chloride substrates with readily reducible functional groups, such as formyl and trifluoromethanesulfonyl groups, were not tolerated

DOI: 10.1021/jacs.6b05712
J. Am. Chem. Soc. 2016, 138, 16266–16273

Table 3. Scope of Dehalogenation Reactions for Aryl Halide Substrates by $[Ce^{III}Cl_6]^{3-}$ Promoted by UVA Light[a]

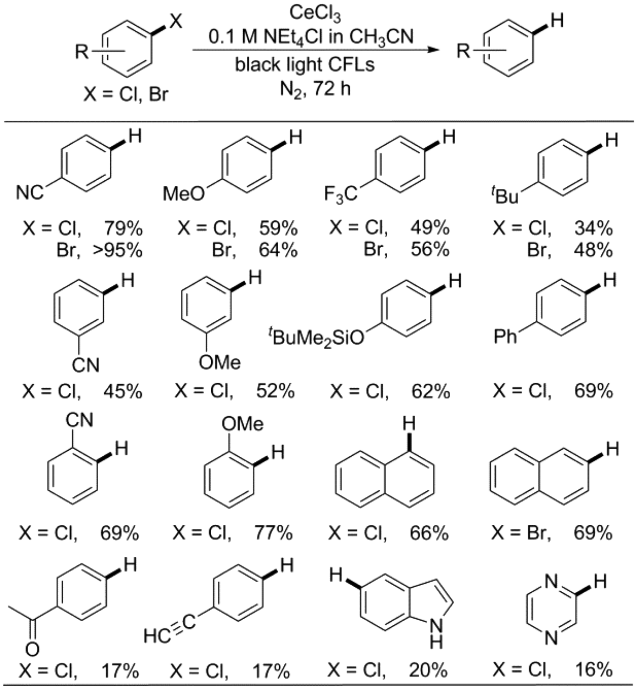

[a]Conditions: 0.2 mmol of substrate, 0.2 mmol of $CeCl_3$, 30 mL CH_3CN solution of 0.1 M NEt_4Cl, irradiated by two 23 W black light compact fluorescent lamps for 72 h. Yields of volatile products were determined by gas chromatography using *n*-dodecane as an internal standard.

under the photochemical reaction conditions, resulting in trace amount of products accompanied by a mixture of unidentified byproducts. The photochemical dehalogenation reaction is not readily applicable in solvents other than CH_3CN, mainly due to the low solubility of $[Ce^{III}Cl_6]^{3-}$ trianion in common organic solvents, including tetrahydrofuran, glyme, and dichloromethane.

Beyond the stoichiometric reduction of aryl chlorides, we sought to take advantage of the complementary oxidative $[Ce^{IV}Cl_6]^{2-}$ photochemistry to close a photocatalytic cycle.[57] The dissociation of a $Cl^{\bullet}$ radical from $[Ce^{IV}Cl_6]^{2-}$ to form $Cl_2^{\bullet-}$ likely occurred upon LMCT excitation and led to the oxidation of the benzylic C−H bonds of toluene as reported by Costanzo and co-workers.[39] Such photoassisted dissociation of chlorine radicals is known for high valent metal chloride complexes, such as $[Pt^{IV}Cl_6]^{2-}$ and $(dppe)Ni^{III}Cl_3$ (dppe = bis-(diphenylphosphino)ethane).[58,59] Thus, when toluene was applied as sacrificial reagent to reduce $[Ce^{IV}Cl_6]^{2-}$ photochemically, the dehalogenation reaction could be carried out for 4-chlorofluorobenzene with 10 mol % $CeCl_3$, yielding fluorobenzene in 66% yield within 3 days (Scheme 2). A higher yield of 78% could be achieved by extending the irradiation time to 6 days. This catalytic reaction can be adapted to aryl chlorides with electron donating and withdrawing substituents, affording dehalogenation products in 46% and 73% yield for 4-methoxyl and 4-cyano substrates, respectively, over the course of 3 days. Such photochemical dehalogenation reactions of aryl halides mediated by $[Ce^{III}Cl_6]^{3-}$ are fundamentally different than those reported for palladium and iron catalysts.[60−62] In the later cases, the reactions likely occurred through initial oxidative addition of carbon halogen bonds to the low valent metal center. These

Scheme 2. Reduction of Aryl Chloride Substrates Using Substoichiometric $[Ce^{III}Cl_6]^{3-}$ under UVA Light

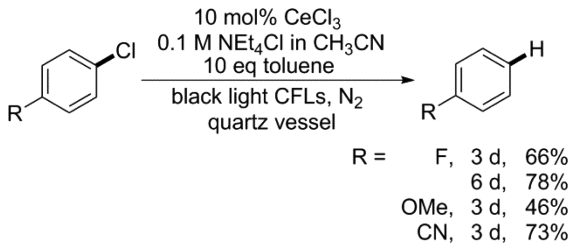

results demonstrate the capability of the $[Ce^{III}Cl_6]^{3-}$ system to access radicals from aryl chlorides through photoredox catalysis.

3. CONCLUSIONS

We have demonstrated that molecular cerium(III) species as simple as $[Ce^{III}Cl_6]^{3-}$ function as photoreductants to mediate organic transformations. The $[Ce^{III}Cl_6]^{3-}$ species was readily accessed by dissolving $CeCl_3$ in CH_3CN in the presence of excess NEt_4Cl. The availability of both $CeCl_3$ and NEt_4Cl salts afforded a simple and inexpensive protocol for applying $[Ce^{III}Cl_6]^{3-}$ anions as photoreductants. Despite a short lifetime of the $^2T_{2g}$* excited state of $[Ce^{III}Cl_6]^{3-}$ of only 22 ns, the low excited-state reduction potential and fast quenching kinetics of $[Ce^{III}Cl_6]^{3-}$ enabled the dehalogenation reactions of Ar−X (X = Cl, Br, I). Divalent f-block element halides, such as SmI_2 have been routinely applied as reductant in a variety of single electron transformations[63,64] due to their availability and low reduction potential. The reported reduction potentials for SmI_2 are −1.41 V versus $Cp_2Fe^{0/+}$ in THF[65] and −2.31 V in the presence of hexamethylphosphoramide (HMPA).[66] However, aryl chloride substrates were noted to be resistant to reduction by SmI_2 even in the presence of HMPA.[64] We expect the use of $CeCl_3$ photochemically in one electron reactions will provide a more potent and readily available f-block element reducing agent than SmI_2. Further efforts toward developing catalytic and tandem C−C bond formation reactions are currently underway in our lab.

It is also noteworthy that the structure and luminescence properties of molecular $[Ce^{III}Cl_6]^{3-}$ species are strongly reminiscent of Ce^{3+} doped elapsolite and $LaCl_3$ solid materials that are used as scintillators in radioluminescence applications.[50,67,68] We expect that inspiration from existing bulk materials will benefit the development of molecular cerium(III) photosensitizers.

4. EXPERIMENTAL SECTION

4.1. General Methods. Unless otherwise indicated all reactions and manipulations were performed under an inert atmosphere (N_2) using standard Schlenk techniques or in a Vacuum Atmospheres, Inc., Nexus II drybox equipped with a molecular sieves 13X/Q5 Cu-0226S catalyst purifier system. Glassware was oven-dried overnight at 150 °C prior to use. ^1H and ^{19}F NMR spectra were obtained on a Bruker DMX-300 Fourier transform NMR spectrometer operating at ^1H frequency of 300 MHz. Elemental analyses were performed at Complete Analysis Laboratories, Inc., using a Carlo Erba EA 1108 analyzer. The qualitative analyses of volatile samples were carried out on an Agilent 5973 inert GC/MS system with a resolution of 0.1 amu for *m*/*z* values using the CI method of ionization. The quantification of volatile samples was conducted on an Agilent 7890A GC system using FID detention method with premade standard curves.

4.2. Optical Spectroscopy. Ten millimeter path length quartz cells fused with a J-Young valve were used to contain samples under a N_2 atmosphere for UV−vis and fluorescence characterizations. Electronic

DOI: 10.1021/jacs.6b05712
J. Am. Chem. Soc. 2016, 138, 16266−16273

absorption spectra (UV−vis) were collected on a PerkinElmer 950 UV−vis/NIR spectrophotometer. Emission and excitation spectra were collected on Fluorolog-3 spectrofluorometer (HORIBA Jobin Yvon, Inc.) using an R928 PMT detector. Deconvolution of the spectra was accomplished with Gaussian functions using fityk.[69] Lifetime measurements were performed on a PTI PicoMaster TCSPC lifetime fluorometer with 340 nm wavelength source. Quantum yields were measured using a comparative method.[70] Quantum yields were calculated against 9,10-diphenylanthracene (Φ_{ST} = 0.97)[71] with following equation:

$$\Phi_x = \Phi_{ST}\left(\frac{\mathrm{Grad}_x}{\mathrm{Grad}_{ST}}\right)\left(\frac{\eta_x^2}{\eta_{ST}^2}\right)$$

where the subscripts ST and x denote the standard (9,10-diphenylanthracene) and sample, respectively. Grad is the gradient obtained from the plot of integrated emission intensity versus absorbance. η is the index of refraction of the solvent. The rate constant for the quenching process of excited-state photosensitizer by externally added quencher, k_q, was obtained using Stern−Volmer relationship:

$$\frac{I^0}{I} - 1 = k_q\tau^0[\mathrm{Q}] = K_{SV}[\mathrm{Q}]$$

where I^0 is the intensity at emission maximum in the absence of quencher, I is the intensity at the emission maximum in the presence of quencher at a concentration of [Q], τ^0 is the lifetime of the photosensitizer in the absence of quencher, K_{SV} (= $k_q\tau^0$) is directly obtained from Stern−Volmer plots as the slope.

4.3. X-ray Crystallography. X-ray reflection intensity data were collected on a Bruker APEXII CCD area detector employing graphite-monochromated Mo Kα radiation (λ = 0.71073 Å) at a temperature of 143(1) K. In all cases, rotation frames were integrated using SAINT,[72] producing a listing of unaveraged F^2 and $\sigma(F^2)$ values, which were then passed to the SHELXTL[73] program package for further processing and structure solution on a Dell Pentium 4 computer. The intensity data were corrected for Lorentz and polarization effects and for absorption using TWINABS[74] or SADABS.[75] The structures were solved by direct methods (SHELXS-97).[76] Refinement was by full-matrix least-squares based on F^2 using SHELXL-97.[76] All reflections were used during refinements. Non-hydrogen atoms were refined anisotropically, and hydrogen atoms were refined using a riding model.

4.4. Electrochemistry. Voltammetry experiments were performed using a CH Instrument 620D electrochemical analyzer/workstation, and the data were processed using CHI software, v9.24. Experiments were performed in a N_2 atmosphere drybox using electrochemical cells that consisted of a 4 mL vial, glassy carbon working electrode, platinum wire counter electrode, and silver wire plated with AgCl as a quasi-reference electrode. The working electrode surfaces were polished prior to each set of experiments. Data were collected in a positive-feedback IR compensation mode at a scan rate of 0.5 V s^{-1}. At the end of the run, cobaltocene was added as internal standard for calibration. The potential of the analyte was reported versus ferrocene.

4.5. Computational Details. *Gaussian 09*, rev. A.02,[77] was used for all electronic structure calculations. The B3LYP hybrid DFT method was employed with a 28-electron small core pseudopotential on cerium with published segmented natural orbital basis set incorporating quasi-relativistic effects[78−80] and the 6-31G* basis set for all other atoms. Gas phase ground-state geometry optimizations for $[Ce^{III}Cl_6]^{3-}$ and $[Ce^{IV}Cl_6]^{2-}$ were carried out with spin states restricted to doublet and singlet for $[Ce^{III}Cl_6]^{3-}$ and $[Ce^{IV}Cl_6]^{2-}$, respectively. The geometry was restricted to octahedral symmetry to afford the most compact orbital representation. The frequency calculations were performed to indicate that the geometries were minima (no imaginary frequencies). TD-DFT calculations were carried out on the optimized geometries of $[Ce^{III}Cl_6]^{3-}$ and $[Ce^{IV}Cl_6]^{2-}$ in the gas-phase.

4.6. Materials. Toluene, Et_2O, and CH_3CN were purchased from Fisher Scientific. The solvents were sparged for 20 min with dry N_2 and dried using a commercial two-column solvent purification system comprising two columns of neutral alumina. Deuterated solvents were purchased from Cambridge Isotope Laboratories, Inc. and stored over molecular sieves overnight (16 h) prior to use. $[NEt_4]_2[Ce^{IV}Cl_6]$ was prepared according to a previous report.[41] $NEt_4Cl{\cdot}H_2O$ was purchased from Alfa Aesar and was used as received. Anhydrous NEt_4Cl was obtained by heating $NEt_4Cl{\cdot}H_2O$ crystalline solids at 100 °C under reduced pressure (<300 mTorr) overnight (16 h). NEt_4Br and NEt_4I were purchased from Acros and Aldrich, respectively, and dried at 100 °C under reduced pressure (<300 mTorr) overnight (16 h) before use.

4.7. Synthesis of $[NEt_4]_3[Ce^{III}Cl_6]$. To a 250 mL Schlenk flask containing $[NEt_4]_2[Ce^{IV}Cl_6]$ (0.700 g, 1.14 mmol, 1.00 equiv) and NEt_4Cl (0.189 g, 1.141 mmol, 1.00 equiv) were added 20 mL of toluene and 80 mL of CH_3CN. The Schlenk flask was sealed under an N_2 atmosphere and irradiated with two 23 W compact fluorescent lamps overnight (16 h) until the yellow solution turned completely colorless. After removal of volatiles, the resulting white solids were extracted with 3 mL of CH_3CN and filtered through Celite packed on a fritted filter. Vapor diffusion of the filtrate with 50 mL of Et_2O resulted in precipitation of colorless crystals. The products were collected on a medium size fritted filter and dried under reduced pressure for 1 h. Yield: 0.687 g, 0.925 mmol, 81%. Elemental analysis found (calculated) for $C_{24}H_{60}Cl_6CeN_3$: C, 38.69 (38.77), H, 8.00 (8.13), N, 5.63 (5.65). Single crystals suitable for X-ray analysis were obtained through the same method but without drying.

4.8. Synthesis of $[NEt_4]_3[Ce^{III}_2Cl_9]$. To a 20 mL scintillation vial containing $CeCl_3$ (0.012 g, 0.050 mmol, 1.00 equiv) suspended in 3 mL of CH_3CN, a 2 mL CH_3CN solution containing $[NEt_4]_3[Ce^{III}Cl_6]$ (0.037 g, 0.050 mmol, 1.00 equiv) was added. After stirring overnight (16 h), the mixture was filtered through a Celite-packed pipette filter. Vapor diffusion of the resulting filtrate with 10 mL of Et_2O led to the precipitation of colorless crystalline materials. The products were collected on a medium porosity size fritted filter and dried under reduced pressure for 1 h. Yield: 0.030 g, 0.030 mmol, 61%. Elemental analysis found (calculated) for $C_{24}H_{60}Ce_2Cl_9N_3$: C, 29.39 (29.12), H, 6.00 (6.11), N, 4.23 (4.24). The connectivity of the anion was established by X-ray studies (Figure S5).

4.9. Synthesis of $[NEt_4]_3[Ce^{III}Br_6]$. To a 20 mL scintillation vial containing $CeBr_3$ (0.038 g, 0.100 mmol, 1.00 equiv) suspended in 5 mL of CH_3CN, a 5 mL CH_3CN solution containing NEt_4Br (0.063 g, 0.300 mmol, 3.00 equiv) was added leading to a color change from pink to colorless. After stirring overnight (16 h), the solution was filtered through a Celite-packed pipet filter. Vapor diffusion of the resulting filtrate with 10 mL of Et_2O led to the precipitation of colorless crystals. The products were collected on a medium size fritted filter and dried under reduced pressure for 1 h. Yield: 0.076 g, 0.075 mmol, 75%. Elemental analysis found (calculated) for $C_{24}H_{60}Br_6CeN_3$: C, 28.50 (28.53), H, 6.25 (5.99), N, 4.19 (4.16). Single crystals suitable for X-ray analysis were obtained through the same method but without drying.

■ ASSOCIATED CONTENT

Supporting Information

The Supporting Information is available free of charge on the ACS Publications website at DOI: 10.1021/jacs.6b05712.

Electrochemical data, electronic absorption data, excitation and emission data, computational details, and optimization data for catalysis (PDF)

Crystallographic data for $[NEt_4]_2[Ce^{IV}Cl_6]$, $[NEt_4]_3[Ce^{III}Cl_6]$, and $[NEt_4]_3[Ce^{III}Br_6]$ (CIF)

■ AUTHOR INFORMATION

Corresponding Authors

*jmanna@sas.upenn.edu

*schelter@sas.upenn.edu

ORCID

Haolin Yin: 0000-0002-2063-8605

Yi Jin: 0000-0002-5633-8305

Eric J. Schelter: 0000-0002-8143-6206

DOI: 10.1021/jacs.6b05712
J. Am. Chem. Soc. 2016, 138, 16266−16273

Notes

The authors declare no competing financial interest.

■ ACKNOWLEDGMENTS

We gratefully acknowledge the University of Pennsylvania and the American Chemical Society Petroleum Research Fund (PRF No. 56128-ND3) for financial support. This work used the Extreme Science and Engineering Discovery Environment (XSEDE), which is supported by U.S. National Science Foundation Grant Number OCI-1053575. The NSF LRSM Research Experiences for Undergraduates (REU) program at UPenn (DMR-1359351) is acknowledged for the financial support of J. E. Hertzog. The Petersson, Chenoweth, and Park groups at the University of Pennsylvania are thanked for use of their fluorometers. The Walsh group at UPenn is acknowledged for the use of their GC. Dr. A. V. Zabula (UPenn) is thanked for providing the quartz reaction vessel.

■ REFERENCES

(1) Prier, C. K.; Rankic, D. A.; MacMillan, D. W. C. *Chem. Rev.* **2013**, *113*, 5322−5363.
(2) Messina, M. S.; Axtell, J. C.; Wang, Y.; Chong, P.; Wixtrom, A. I.; Kirlikovali, K. O.; Upton, B. M.; Hunter, B. M.; Shafaat, O. S.; Khan, S. I.; Winkler, J. R.; Gray, H. B.; Alexandrova, A. N.; Maynard, H. D.; Spokoyny, A. M. *J. Am. Chem. Soc.* **2016**, *138*, 6952−6955.
(3) Jouffroy, M.; Primer, D. N.; Molander, G. A. *J. Am. Chem. Soc.* **2016**, *138*, 475−478.
(4) Tellis, J. C.; Primer, D. N.; Molander, G. A. *Science* **2014**, *345*, 433−436.
(5) Xi, Y.; Yi, H.; Lei, A. *Org. Biomol. Chem.* **2013**, *11*, 2387−2403.
(6) Zeitler, K. *Angew. Chem., Int. Ed.* **2009**, *48*, 9785−9789.
(7) Xuan, J.; Xiao, W.-J. *Angew. Chem., Int. Ed.* **2012**, *51*, 6828−6838.
(8) Hari, D. P.; König, B. *Angew. Chem., Int. Ed.* **2013**, *52*, 4734−4743.
(9) Kindt, S.; Heinrich, M. R. *Synthesis* **2016**, *48*, 1597−1606.
(10) Li, L.; Liu, W.; Zeng, H.; Mu, X.; Cosa, G.; Mi, Z.; Li, C.-J. *J. Am. Chem. Soc.* **2015**, *137*, 8328−8331.
(11) Zhang, H.; Zhu, R.-S.; Wang, G.-J.; Han, K.-L.; He, G.-Z.; Lou, N.-Q. *J. Chem. Phys.* **1999**, *110*, 2922−2927.
(12) Tang, B.; Zhu, R.; Tang, Y.; Ji, L.; Zhang, B. *Chem. Phys. Lett.* **2003**, *381*, 617−622.
(13) Thekaekara, M. P. *Sol. Energy* **1976**, *18*, 309−325.
(14) Schultz, D. M.; Yoon, T. P. *Science* **2014**, *343*, 1239176.
(15) Nguyen, J. D.; D'Amato, E. M.; Narayanam, J. M. R.; Stephenson, C. R. J. *Nat. Chem.* **2012**, *4*, 854−859.
(16) Koike, T.; Akita, M. *Inorg. Chem. Front.* **2014**, *1*, 562−576.
(17) Che, C.-M.; Kwong, H.-L.; Yam, V. W.-W.; Cho, K.-C. *J. Chem. Soc., Chem. Commun.* **1989**, 885−886.
(18) Li, D.; Che, C.-M.; Kwong, H.-L.; Yam, V. W.-W. *J. Chem. Soc., Dalton Trans.* **1992**, 3325−3329.
(19) Revol, G.; McCallum, T.; Morin, M.; Gagosz, F.; Barriault, L. *Angew. Chem., Int. Ed.* **2013**, *52*, 13342−13345.
(20) Creutz, S. E.; Lotito, K. J.; Fu, G. C.; Peters, J. C. *Science* **2012**, *338*, 647−651.
(21) Tan, Y.; Munoz-Molina, J. M.; Fu, G. C.; Peters, J. C. *Chem. Sci.* **2014**, *5*, 2831−2835.
(22) Uyeda, C.; Tan, Y.; Fu, G. C.; Peters, J. C. *J. Am. Chem. Soc.* **2013**, *135*, 9548−9552.
(23) Ziegler, D. T.; Choi, J.; Muñoz-Molina, J. M.; Bissember, A. C.; Peters, J. C.; Fu, G. C. *J. Am. Chem. Soc.* **2013**, *135*, 13107−13112.
(24) Pause, L.; Robert, M.; Savéant, J.-M. *J. Am. Chem. Soc.* **1999**, *121*, 7158−7159.
(25) Harkins, S. B.; Peters, J. C. *J. Am. Chem. Soc.* **2005**, *127*, 2030−2031.
(26) Sattler, W.; Ener, M. E.; Blakemore, J. D.; Rachford, A. A.; LaBeaume, P. J.; Thackeray, J. W.; Cameron, J. F.; Winkler, J. R.; Gray, H. B. *J. Am. Chem. Soc.* **2013**, *135*, 10614−10617.
(27) Yin, H.; Carroll, P. J.; Manor, B. C.; Anna, J. M.; Schelter, E. J. *J. Am. Chem. Soc.* **2016**, *138*, 5984−5993.
(28) Ghosh, I.; Ghosh, T.; Bardagi, J. I.; König, B. *Science* **2014**, *346*, 725−728.
(29) Discekici, E. H.; Treat, N. J.; Poelma, S. O.; Mattson, K. M.; Hudson, Z. M.; Luo, Y.; Hawker, C. J.; de Alaniz, J. R. *Chem. Commun.* **2015**, *51*, 11705−11708.
(30) Yin, H.; Carroll, P. J.; Anna, J. M.; Schelter, E. J. *J. Am. Chem. Soc.* **2015**, *137*, 9234−9237.
(31) Montini, T.; Melchionna, M.; Monai, M.; Fornasiero, P. *Chem. Rev.* **2016**, *116*, 5987−6041.
(32) Piro, N. A.; Robinson, J. R.; Walsh, P. J.; Schelter, E. J. *Coord. Chem. Rev.* **2014**, *260*, 21−36.
(33) Vogler, A.; Kunkely, H. *Inorg. Chim. Acta* **2006**, *359*, 4130−4138.
(34) Stevenson, S. M.; Shores, M. P.; Ferreira, E. M. *Angew. Chem., Int. Ed.* **2015**, *54*, 6506−6510.
(35) Higgins, R. F.; Fatur, S. M.; Shepard, S. G.; Stevenson, S. M.; Boston, D. J.; Ferreira, E. M.; Damrauer, N. H.; Rappé, A. K.; Shores, M. P. *J. Am. Chem. Soc.* **2016**, *138*, 5451−5464.
(36) Sattler, W.; Henling, L. M.; Winkler, J. R.; Gray, H. B. *J. Am. Chem. Soc.* **2015**, *137*, 1198−1205.
(37) Kern, J.-M.; Sauvage, J.-P. *J. Chem. Soc., Chem. Commun.* **1987**, 546−548.
(38) Xiang, H.; Cheng, J.; Ma, X.; Zhou, X.; Chruma, J. J. *Chem. Soc. Rev.* **2013**, *42*, 6128−6185.
(39) Costanzo, L. L.; Pistarà, S.; Condorelli, G. *J. Photochem.* **1983**, *21*, 45−51.
(40) Shannon, R. *Acta Crystallogr., Sect. A: Cryst. Phys., Diffr., Theor. Gen. Crystallogr.* **1976**, *32*, 751−767.
(41) Löble, M. W.; Keith, J. M.; Altman, A. B.; Stieber, S. C. E.; Batista, E. R.; Boland, K. S.; Conradson, S. D.; Clark, D. L.; Lezama Pacheco, J.; Kozimor, S. A.; Martin, R. L.; Minasian, S. G.; Olson, A. C.; Scott, B. L.; Shuh, D. K.; Tyliszczak, T.; Wilkerson, M. P.; Zehnder, R. A. *J. Am. Chem. Soc.* **2015**, *137*, 2506−2523.
(42) Pohako-Esko, K.; Wehner, T.; Schulz, P. S.; Heinemann, F. W.; Müller-Buschbaum, K.; Wasserscheid, P. *Eur. J. Inorg. Chem.* **2016**, *2016*, 1333−1339.
(43) Blasse, G.; Bril, A. *J. Chem. Phys.* **1967**, *47*, 5139−5145.
(44) Hazin, P. N.; Bruno, J. W.; Brittain, H. G. *Organometallics* **1987**, *6*, 913−918.
(45) Hazin, P. N.; Lakshminarayan, C.; Brinen, L. S.; Knee, J. L.; Bruno, J. W.; Streib, W. E.; Folting, K. *Inorg. Chem.* **1988**, *27*, 1393−1400.
(46) Rausch, M. D.; Moriarty, K. J.; Atwood, J. L.; Weeks, J. A.; Hunter, W. E.; Brittain, H. G. *Organometallics* **1986**, *5*, 1281−1283.
(47) Zheng, X.-L.; Liu, Y.; Pan, M.; Lü, X.-Q.; Zhang, J.-Y.; Zhao, C.-Y.; Tong, Y.-X.; Su, C.-Y. *Angew. Chem., Int. Ed.* **2007**, *46*, 7399−7403.
(48) Ryan, J. L.; Jørgensen, C. K. *J. Phys. Chem.* **1966**, *70*, 2845−2857.
(49) Laroche, M.; Bettinelli, M.; Girard, S.; Moncorgé, R. *Chem. Phys. Lett.* **1999**, *311*, 167−172.
(50) Tanner, P. A.; Mak, C. S. K.; Edelstein, N. M.; Murdoch, K. M.; Liu, G.; Huang, J.; Seijo, L.; Barandiarán, Z. *J. Am. Chem. Soc.* **2003**, *125*, 13225−13233.
(51) Rehm, D.; Weller, A. *Isr. J. Chem.* **1970**, *8*, 259−271.
(52) Tucker, J. W.; Stephenson, C. R. J. *J. Org. Chem.* **2012**, *77*, 1617−1622.
(53) Izutsu, K. *Electrochemistry in Nonaqueous Solutions*; Wiley-VCH Verlag GmbH & Co. KGaA: Weinheim, Germany, 2003, p 105.
(54) Grimshaw, J. *Electrochemical reactions and mechanisms in organic chemistry*; Elsevier Science B. V.: Amsterdam, 2000, p 99.
(55) Cismesia, M. A.; Yoon, T. P. *Chem. Sci.* **2015**, *6*, 5426−5434.
(56) Connelly, N. G.; Geiger, W. E. *Chem. Rev.* **1996**, *96*, 877−910.
(57) Since two photons are needed for turning over the catalytic cycle, the theoretical photon efficiency for the catalytic reaction is limited to a maximum of 50%.
(58) Grivin, V. P.; Khmelinski, I. V.; Plyusnin, V. F.; Blinov, I. I.; Balashev, K. P. *J. Photochem. Photobiol., A* **1990**, *51*, 167−178.
(59) Hwang, S. J.; Powers, D. C.; Maher, A. G.; Anderson, B. L.; Hadt, R. G.; Zheng, S.-L.; Chen, Y.-S.; Nocera, D. G. *J. Am. Chem. Soc.* **2015**, *137*, 6472−6475.

DOI: 10.1021/jacs.6b05712
J. Am. Chem. Soc. 2016, 138, 16266−16273

(60) Viciu, M. S.; Grasa, G. A.; Nolan, S. P. *Organometallics* **2001**, *20*, 3607−3612.
(61) Czaplik, W. M.; Grupe, S.; Mayer, M.; Wangelin, A. J. v. *Chem. Commun.* **2010**, *46*, 6350−6352.
(62) Chen, J.; Zhang, Y.; Yang, L.; Zhang, X.; Liu, J.; Li, L.; Zhang, H. *Tetrahedron* **2007**, *63*, 4266−4270.
(63) Szostak, M.; Fazakerley, N. J.; Parmar, D.; Procter, D. J. *Chem. Rev.* **2014**, *114*, 5959−6039.
(64) Procter, D. J.; Flowers, R. A.; Skrydstrup, T. *Organic Synthesis Using Samarium Diiodide: A Practical Guide*. Royal Society of Chemistry: Cambridge, U.K., 2010, p 17.
(65) Dahlén, A.; Nilsson, Å.; Hilmersson, G. *J. Org. Chem.* **2006**, *71*, 1576−1580.
(66) Szostak, M.; Spain, M.; Procter, D. J. *J. Org. Chem.* **2014**, *79*, 2522−2537.
(67) Kramer, K. W.; Dorenbos, P.; Gudel, H. U.; van Eijk, C. W. E. *J. Mater. Chem.* **2006**, *16*, 2773−2780.
(68) Dorenbos, P. *J. Lumin.* **2000**, *91*, 91−106.
(69) Wojdyr, M. *J. Appl. Crystallogr.* **2010**, *43*, 1126−1128.
(70) Lakowicz, J. R. *Principles of Fluorescence Spectroscopy*; Springer: New York, 2007, pp 54−55.
(71) Suzuki, K.; Kobayashi, A.; Kaneko, S.; Takehira, K.; Yoshihara, T.; Ishida, H.; Shiina, Y.; Oishi, S.; Tobita, S. *Phys. Chem. Chem. Phys.* **2009**, *11*, 9850−9860.
(72) *SAINT*; Bruker AXS Inc.: Madison, WI, 2009.
(73) *SHELXTL*; Bruker AXS Inc.: Madison, WI, 2009.
(74) Sheldrick, G. M. *TWINABS*; University of Gottingen: Gottingen, Germany, 2008.
(75) Sheldrick, G. M. *SADABS*; University of Gottingen: Gottingen, Germany, 2007.
(76) Sheldrick, G. M. *Acta Crystallogr., Sect. A: Found. Crystallogr.* **2008**, *64*, 112−122.
(77) Frisch, M. J.; Trucks, G. W.; Schlegel, H. B.; Scuseria, G. E.; Robb, M. A.; Cheeseman, J. R.; Scalmani, G.; Barone, V.; Mennucci, B.; Petersson, G. A.; Nakatsuji, H.; Caricato, M.; Li, X.; Hratchian, H. P.; Izmaylov, A. F.; Bloino, J.; Zheng, G.; Sonnenberg, J. L.; Hada, M.; Ehara, M.; Toyota, K.; Fukuda, R.; Hasegawa, J.; Ishida, M.; Nakajima, T.; Honda, Y.; Kitao, O.; Nakai, H.; Vreven, T.; Montgomery, J. A., Jr.; Peralta, J. E.; Ogliaro, F.; Bearpark, M.; Heyd, J. J.; Brothers, E.; Kudin, K. N.; Staroverov, V. N.; Kobayashi, R.; Normand, J.; Raghavachari, K.; Rendell, A.; Burant, J. C.; Iyengar, S. S.; Tomasi, J.; Cossi, M.; Rega, N.; Millam, J. M.; Klene, M.; Knox, J. E.; Cross, J. B.; Bakken, V.; Adamo, C.; Jaramillo, J.; Gomperts, R.; Stratmann, R. E.; Yazyev, O.; Austin, A. J.; Cammi, R.; Pomelli, C.; Ochterski, J. W.; Martin, R. L.; Morokuma, K.; Zakrzewski, V. G.; Voth, G. A.; Salvador, P.; Dannenberg, J. J.; Dapprich, S.; Daniels, A. D.; Farkas, O.; Foresman, J. B.; Ortiz, J. V.; Cioslowski, J.; Fox, D. J. *Gaussian 09*, revision A.02; Gaussian, Inc.: Wallingford, CT, 2009.
(78) Cao, X.; Dolg, M. *J. Mol. Struct.: THEOCHEM* **2004**, *673*, 203−209.
(79) Cao, X.; Dolg, M.; Stoll, H. *J. Chem. Phys.* **2003**, *118*, 487−496.
(80) Küchle, W.; Dolg, M.; Stoll, H.; Preuss, H. *J. Chem. Phys.* **1994**, *100*, 7535−7542.

DOI: 10.1021/jacs.6b05712
J. Am. Chem. Soc. 2016, 138, 16266−16273